LHCb Collaboration

LHCb 2007-115

August 2007

Results of the MWPC gas gain uniformity tests performed at CERN

A. Alves, A. F. Barbosa, G. Guerrer, H. P. Lima Jr., A. Reis
Centro Brasileiro de Pesquisas Físicas - CBPF
Luciano M. de Andrade Filho
COPPE - UFRJ
E. Polycarpo, F. Rodrigues, C. Schoch Vianna
Instituto de Física - UFRJ*
J.S. Graulich, K. Mair, B. Schmidt, T. Schneider
CERN

Abstract

We present the results of the gas gain uniformity tests performed as part of the quality control of the multiwire proportional chambers produced at CERN for the LHCb Muon system, along with a description of the last hardware and software upgrades. The test provides a relative gas gain measurement over the whole chamber sensitive area. It is based on the analysis of the spectrum obtained when the chamber is exposed to a ^{241}Am radioactive source. Since the measurement is normalized to the peak of a precise pulse generator, the gain uniformity can also be evaluated among different gas gaps and different chambers.

*This work has been partially supported by CNPq and Fundação Universitária José Bonifácio (FUJB)

Contents

1 Introduction **2**

2 Overview of the Experimental Setup **3**
2.1 Readout Scheme 3
2.2 Data Acquisition and Data Analysis 4

3 Test Station Hardware Upgrade **4**
3.1 The new pre-amplifier circuit 5
3.2 The Data Processing Module (DPM) 6
3.3 The Data Acquisition Software 8

4 Results **10**
4.1 Classification 10
4.2 HV dependency and correction 13
4.3 Statistics 15

5 Conclusions **16**

Appendix **18**

1 Introduction

The purpose of the LHCb Muon System [1,2] is to provide fast (L0) triggering and offline muon identification. The system is made of five stations (M1-M5) of rectangular shape, covering an acceptance of $\pm$300 mrad (horizontally) and $\pm$250 mrad (vertically). Four stations of the muon system (M2-M5) are placed after the Hadron Calorimeter (HCAL) and are interleaved with thick iron walls. M1 is placed in front of the SPD/PS (Scintillator Pad Detector/Preshower). Each station is divided in four regions (R1- R4), with increasing distance from the beam axis, defining increasing angles from the interaction point.

The first station is equipped with Gas Electron Multiplier (GEM) chambers in R1 and with two-gap Multi-Wire Proportional Chambers (MWPC) in the other regions. The other stations are equipped with four-gap MWPC with 2 mm wire spacing and a small gas gap (5 mm). In total, the system is composed of 1368 MWPC, of 20 different sizes, with either anode or cathode readout, or even simultaneous cathode and anode readout. 134 chambers of the following regions have been built at CERN: M2R1, M2R2, M3R1, M3R2, M4R1 and M5R1. These chambers can be divided in three different groups according to their design. M1R2 chambers are in Group I: it is a double gap chamber with cathode readout. M2 and M3 chambers are classified in Group II. They are 4-gap chambers with cathode and wire readout. Finally, Group III comprises the M4 and M5 chambers, which are 4-gap chambers with cathode readout. Table 1 summarizes the design parameters of these detectors.

Table 1: Chamber classification according to different readout designs. Numbers are taken from [3].

	Group	# of Chambers	Sensitive area (mm^2)	# of Wire pads and width (mm)	# of Cathode pads and area (mm^2)	# of FE boards per chamber
M1R2	I	24	240×200		24×8 10×25	12
M2R1	II	12	308×253	48 6.3	8×8 37.5×31.3	14
M2R2	II	24	612×253	48 12.5	8×8 75×31.3	14
M3R1	II	12	332×273	24 6.7	8×8 40.5×33.7	14
M3R2	II	24	660×273	48 13.5	8×8 80×33.7	14
M4R1	III	12	356×293		12×8 29×36	12
M5R1	III	12	380×313		12×8 31×39	12

Figure 1 shows a schematic view of a typical 4-gap LHCb muon chamber, with details of the readout connections in the cathode and anode planes. In each gap, the anode signals are read out at one side of the chamber (see Figure 1 (c)), while the cathode readout connections are divided in two halves, one in each side (see Figure 1 (b)).

In order to guarantee a constant quality of the produced chambers and to allow fast tracing of potential production problems, precise procedures have been defined for each production step. In addition, six main quality control tests are performed at different stages of the production: wire

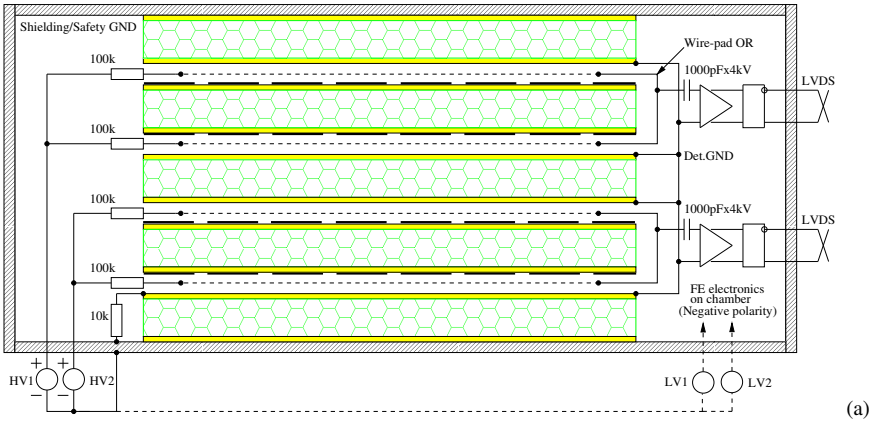

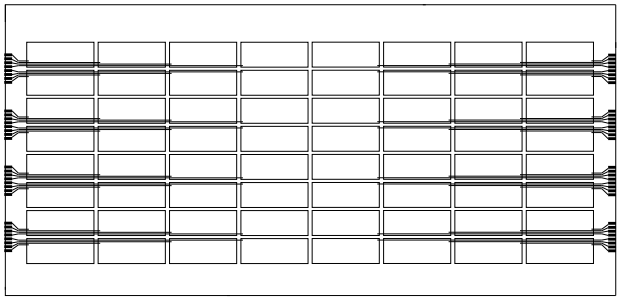

(b)

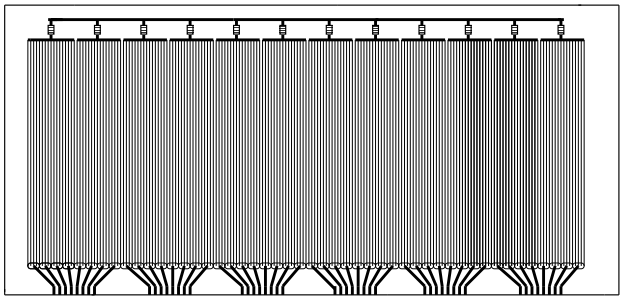

(c)

Figure 1: Schematic view of a MWPC, showing 4 gas gaps (a). Readout connections from the cathode pads (b) and from anode plane (c).

fixation bar thickness, wire pitch, wire tension, gas leak rate, dark current and gas gain uniformity. The first five of them have been presented in [4]. This note presents the results obtained for the gas gain uniformity tests applied to all CERN produced chambers, except the ones produced for the first station (M1R2), where the proposed measurement method could not be applied.

2 Overview of the Experimental Setup

The gas gain uniformity measurement is based on the analysis of the pulse height spectrum obtained when the chamber is exposed to an ^{241}Am radioactive source. This spectrum exhibits a peak at a position proportional to the gas gain. This peak, which is used as a reference, results mainly from the absorption of fluorescence X-rays emitted by the copper atoms of the cathode plane when excited by the 60 keV gamma rays coming from the source. It is degraded by the relatively poor energy resolution of the chamber and the superposition with the Compton spectrum of the 60 keV γ-rays. The gamma activity of the source (24 MBq) is low enough to minimize radiation safety issues and the small size of the chambers allows the fixation of the source over the chamber in a central position where it is possible to illuminate the whole chamber.

2.1 Readout Scheme

While the pulse height spectrum is obtained from the anode wires signal, the cathode pads readout is used for localizing the X-ray photons on the gap plane. Each cathode pad of one half of a gap (see

Figure 1 (b)) is connected to a different cell of a delay line. The delay line is read out at both ends. By comparing the arrival times of the cathode signal at each end of the delay line, the cathode pad position is identified. In this way only two pre-amplifiers are needed to read out a half gap. These signals are then discriminated and the time difference between the signals from the two delay line outputs is digitized. To retrieve the pulse height information all anode wire signals of one gap are short circuited and amplified in one readout channel. The amplitude of the anode signal is digitized. The data acquisition system provides a way to synchronize for each event occurring in the chamber the time information and the pulse amplitudes obtained from the cathodes and the wires, respectively. In that way the amplitude spectrum can be plotted for each pad of any of the four chamber gas gaps.

Fig. 2 shows a schematic view of the test station readout stages for one gap. The anode bar is a printed circuit board which provides the short-circuit of the whole anode wire plane. The anode signal is split in two after amplification so that it can be simultaneously discriminated and analysed into an analog-to-digital converter (ADC). The digital signals from the output of the discriminators are input to a time-to-digital converter (TDC), as start (anode) or stop signals (cathode). In order to read out all the 4 gaps, we use 8 delay lines and 16 amplifiers for the cathode signals and 4 amplifiers for the anode signals, as well as 20 discriminator channels. The hardware modules used up to this point comprise what we call the analog part of the data readout. The whole system is assembled on a metallic surface which is also the ground plane. In addition, low voltage power supplies are required to provide the +12V and -12V to the station, and a high voltage power supply is needed for the wire chamber operation. The Data AcQuisition system (DAQ) is shown as a box containing the TDC, the ADC, and a controller which communicates to a personal computer. A picture of the setup can be seen in Figure 3, where the main stages of the analog part of the signal readout are indicated.

The test station based on these principles has been proposed in [5] and developed along the years 2004-2005. A detailed description is presented in [6], together with some characterization tests. The first results were published in [4].

2.2 Data Acquisition and Data Analysis

Although the method used to test the gas gain uniformity has been kept the same over all CERN chamber tests, the implementation of the data acquisition system has evolved. After a short period during which the test station has been operated with commercial TDC and ADC modules based on the VME standard and data analysis performed offline using PAW [7], a dedicated hardware using dual ADC and TDC integrated circuits has been developed and implemented. A field programmable gate array (FPGA) has been introduced to manage the data flow control and storage. The associated software runs under MS-Windows on any PC with parallel port communication, replacing the previously used PVSS and VME servers. It incorporates the capability of analyzing the acquired data and of providing a complete report on chamber characterization items. Table 2 shows which chambers were tested with the DAQ based on the VME standard and which were tested with the new Data Processing Module (DPM) described in Sec. 3.

3 Test Station Hardware Upgrade

The improvements made to the test station during 2004-2005 consist mainly of a new pre-amplifier for the cathode signals read out from the delay lines, the new DAQ and the analysis software. These are described in the following sections:

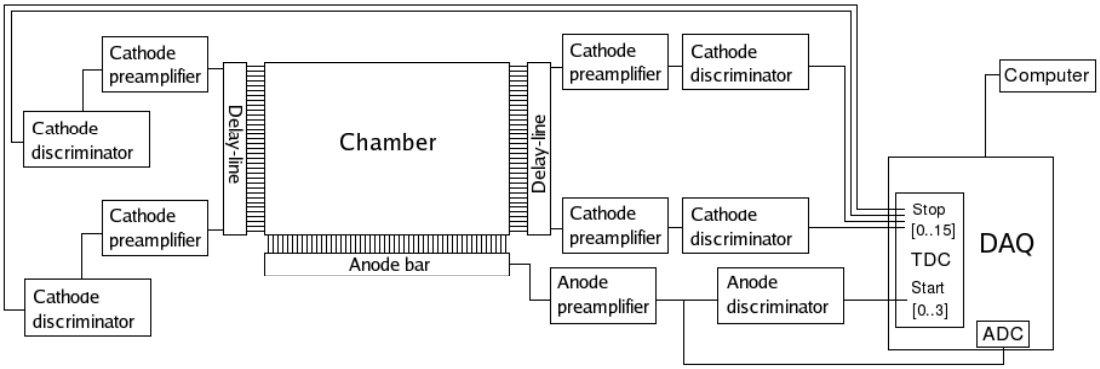

Figure 2: Schematic view of the test station setup.

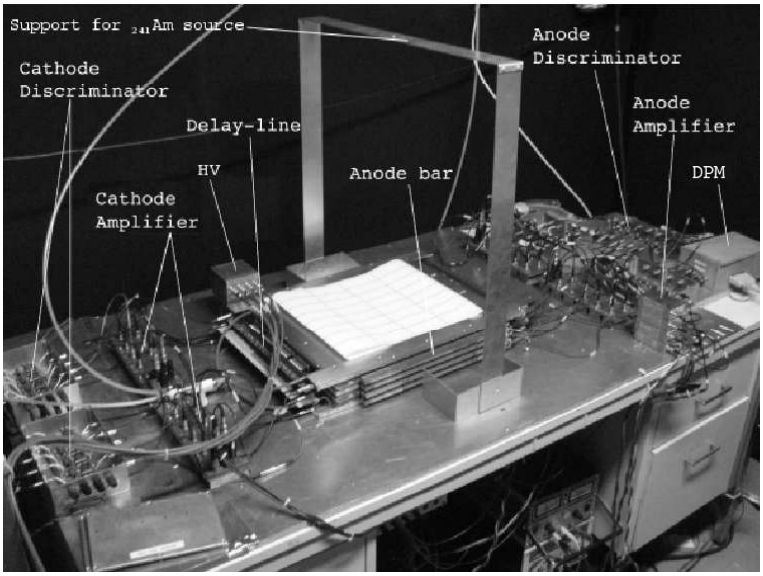

Figure 3: Picture of the test station setup, indicating the delay line, the cathode amplifiers and discriminators in one side of the station. The other side is analog. When in use, the radioactive source is placed on the aluminum support, above the chamber center. Here the DAQ system shown is the new Data Processing Module developed at CBPF (see Section 3. The first setup used a VME crate for the DAQ modules.

Table 2: DAQ system used in the gas gain uniformity tests of each chamber type.

Chamber Type	DAQ
M2R1	DPM
M2R2	DPM / VME
M3R1	VME
M3R2	VME
M4R1	DPM
M5R1	DPM

3.1 The new pre-amplifier circuit

The previous pre-amplifier circuit design [6] relied on an input stage featuring low gain and high input impedance, followed by a series of low gain wide band pass identical stages, and a unity gain low

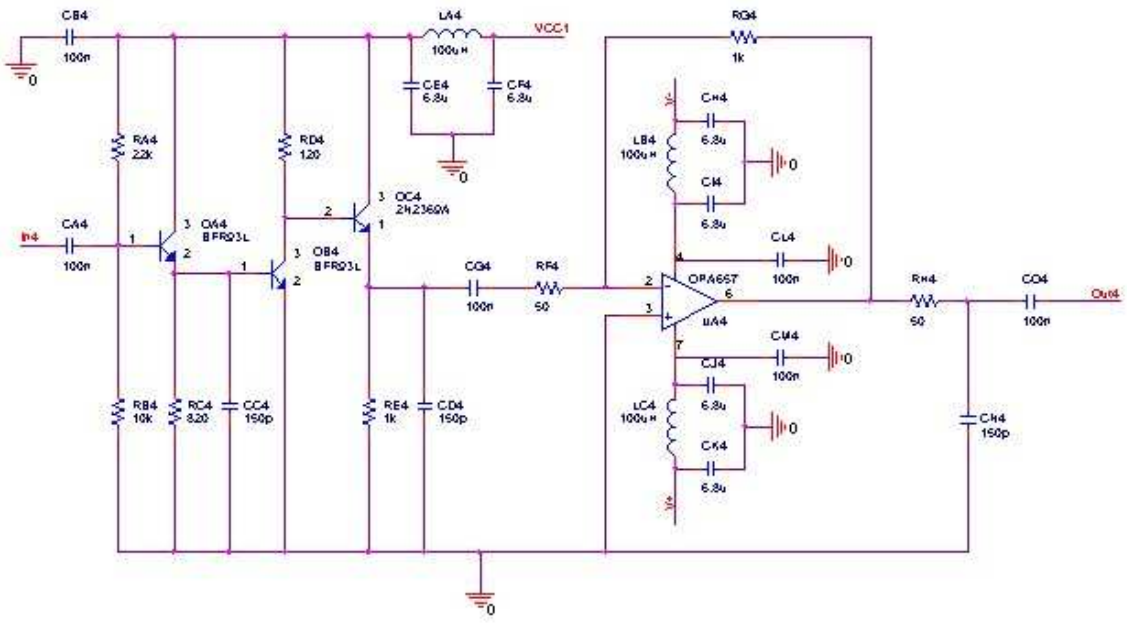

Figure 4: The pre-amplifier circuit diagram.

output impedance driver stage. This concept was applied with off-the-shelf discrete transistors, which implied a relatively complex circuitry with modest performance. In the new circuit, the same concept is used with a higher performance transistor (BFR93A) both at the input and gain stages. In addition, a low noise wide-band operational amplifier [8] is used at the output stage, providing an extra gain of a factor 20. The anode and cathode signal spectral composition has been analyzed, and some filtering has been added to the circuit in order to match its band pass to these signals, so that an improved signal-to-noise ratio is obtained and the rise time is kept below 25ns. A complete description of the pre-amplifier development may be found in [9]. Figure 4 is a scheme of the implemented circuit.

3.2 The Data Processing Module (DPM)

The Data Processing Module is a custom system designed to acquire data from the muon chambers and to perform the identification of the pad being hit by an ionizing event, as well as the pulse amplitude related to this event. Both capabilities are implemented in one four-layer printed circuit board, controlled by standalone software. The data readout is done by a standard PC, using the Enhanced Parallel Port (EPP) Interface. Figure 5 is a general schematic view of the DPM. The digitizer block basically consists of two dual pipeline analog-to-digital converters that provide samples of the input (anode) pulse to the digital peak-detector block. The output of the peak-detector is multiplexed, depending on which gap registered the event.

The coincidence logic triggers the peak detector whenever any of the four start pulses is received from the readout electronics. It also triggers the event builder block if the corresponding event is considered as valid. An event is valid if it is associated to the detection of a photon from a radiation source, i.e., if it occurs in only one gap (see Section 3.2). A crossing muon, for example, would leave its track in more than one gap, and would be rejected. The goal of the coincidence logic is to allow for the use of only 2 TDC channels instead of using 16 (one for each cathode readout channel), as

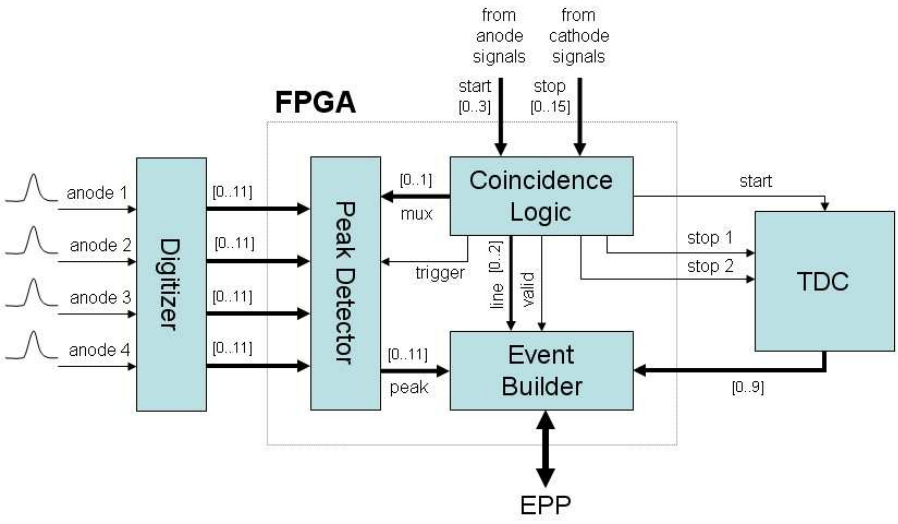

Figure 5: DPM functional block diagram.

implemented in the previous version of the test station [6]. The coincidence logic block also identifies the delay line (cathode) and the gap (anode) where the valid event has occurred in the chamber. The event builder assembles all the relevant information about the event and sends it to the PC. The event information includes the delay line identification, the time measurement information, and the pulse amplitude found by the peak-detector. Except for the Digitizer and the TDC blocks, the whole design has been developed in VHDL and implemented in a single FPGA.

The Digitizer

The anode analog signals are converted to digital in the Digitizer block and sent for further processing within the FPGA. The Digitizer block consists of four identical channels, each one composed of a low distortion differential driver and a fast pipeline ADC [10]. The single-ended signal coming from the pre-amplifier is first converted to differential mode in order to achieve optimum performance of the ADC. Operation in differential mode reduces distortion in the ADC when compared to single-ended operation, especially at high sampling rates. A low distortion differential driver has been selected to perform the single-to-differential conversion. This driver [11] is recommended by the ADC manufacturer as a good choice to achieve low harmonic distortion, balanced output gain and phase matching in the outputs. In order to perform analog-to-digital conversion, a dual ADC has been chosen (AD9238BST-65, [10]). This is a free-running converter that features a high performance sample-and-hold amplifier and uses a multi-stage differential pipelined architecture with output error correction logic. This ADC provides 12-bit resolution at 65 MSPS (mega samples per second), with 600 mW power consumption. The ADC operates with a clock signal generated by the FPGA through the use of an external crystal oscillator and a Phase Locked Loop (PLL) block. The analog-to-digital conversion can be disabled through a power-down input controlled by the FPGA. When enabled, each ADC continuously delivers a digitized stream of the anode signal to the Peak Detector block.

The Peak Detector

The peak detector searches the highest sample value converted by the ADC in a time window of 500 ns. This window is adequate to the shape of the typical anode pulse. A state machine mechanism has

been implemented in the peak-detector circuit in order to seek for the peak in the input word. This mechanism is triggered by a signal generated in the coincidence logic block.

Coincidence logic

An event selection logic circuit has been implemented to filter out the background noise due to casual events and to decrease the number of TDC channels required for data acquisition. Valid events originating from the X-ray ^{241}Am source only occur in one of the chamber gaps, where the photo-electric effect has taken place. Since only one delay line (cathode) is expected to propagate the valid event, provided that the delay line identification is properly registered, one can use the same TDC channel for all delay lines, doing an OR logic in the discriminator outputs. This feature plus an internal look-up table, which encodes valid events among all possible input combinations, are the main facilities implemented in this block.

TDC block

The TDC block is composed of one integrated circuit, the TDC F1 [12]. This time-to-digital converter was initially developed to be used in the COMPASS experiment at CERN [13]. It has 8 conversion channels and 120 picoseconds resolution in each channel. The resolution is adjusted by software and calibrated by a quartz crystal using a PLL circuit. One start signal is common to all the other (stop) channels. In the mode under which the TDC F1 has been configured in the DPM, its maximum data processing rate can reach 2 million events per second. This TDC is controlled through its configuration registers, and the configuration procedure is done by a serial bit stream using a specific protocol. In the current application, this protocol was implemented by software sending the correct bit stream via the registers implemented in the FPGA. Only two F1 channels are used by the test station, as explained in Section 3.2.

3.3 The Data Acquisition Software

The MUon CHamber software (MUCH 1.0) allows all the test procedure to be performed by a single executable file. Its graphical user interface (GUI) provides a user-friendly and intuitive going-through mechanism to execute the steps necessary to test a muon chamber. These steps are summarized here and explained in more details in the next sub-sections.

The MUCH software is available in two versions: one for chambers with 64 pads per gap and another one for those with 96 pads per gap. Figure 6 is a capture of the main window for chambers with 64 pads. From this window one can access any feature implemented in the software. If the hardware is not connected to the computer, some functions related to data acquisition are kept disabled. A message on the bottom-left corner of the main window informs whether the DPM hardware is connected and has been detected by the computer.

In the main window of the MUCH software, the following elements are seen:

- A toolbar with the main available menus File, View, Acquire and Analysis;
- A secondary toolbar containing shortcuts to frequently used commands;
- An auxiliary window called Acquisition Status, which presents information on the current data acquisition or loaded file (not enabled in 6) ;

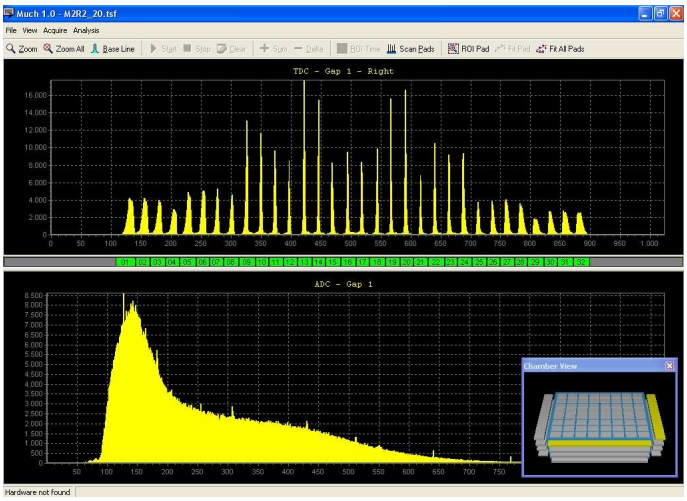

Figure 6: Capture of the main window of the MUCH software (64-pad chambers).

- An auxiliary window called Chamber View, showing a graphic view of the chamber under test;
- Two main graphic windows, one for the timing spectrum (top), and the other one for the pulse amplitude spectrum (bottom).

The functions available through the menus in the main toolbar are explained in the next paragraphs. The Acquisition Status window is used to show updated information about the current acquisition. This information comprises: Acquisition time (for how long the current acquisition is active), rate of events processed by the DPM, number of events already processed for the active gap, and the total number of events for all the gaps. The Chamber View window allows one to choose the active gap and the active pad viewed on the screen. This is done by left-clicking the mouse button in the desired object.

The timing spectrum is presented in the graphic window at the top (TDC window). At the bottom of this graphic, one can see square objects numbered from left to right. These objects are used to define the time interval limits related to each peak that corresponds to one pad in the chamber. The bottom graphic window (ADC window) shows the amplitude measurements histogram, i.e., the distribution of amplitudes measured for the anode signals during the data acquisition interval.

All the procedures required to test a MWPC are described in detail in the appendix. Instructions on how to operate the software, from data acquisition to analysis and report generation, are also given. It is important to note, however, that at the end of a test run, the user can proceed analysing the data using the same software, i.e., to get the final results for the gas gain uniformity over the four gaps surfaces of a chamber. Since the gain is given by the normalized (see appendix) value of the gaussian mean value fitted to the amplitude spectrum of each individual pad, different views of all the parameters related to this fit are provided. The main plots shown in the test report are:

- Normalized gas gain as a function of the pad number (Figure 8(a));
- The histogram of the gas gain in each gap (Figure 8(b));
- Two-dimensional distribution of the normalized gas gain (Figure 8(c));
- Three-dimensional view of the gas gain distribution in each gap (Figure 8(d));

- The time spectrum of the cathode signals in the right (Figure 7(a)) and left (Figure 7(b)) side of each gap;
- The global amplitude spectrum in each gap (Figure 7(c));
- Fitted peak width as a function of the pad number in each gap (Figure 8(e));
- χ^2 of the Gaussian fits as a function of the pad number in each gap (Figure 8(f));
- Error on the peak mean value as a function of the pad number (Figure 8(g));
- Error on the peak width as a function of the pad number (Figure 8(h)).

The normalized gas gain in all the pads in one chamber is also saved in a text file, which is used to perform the global analysis of all the gas gain uniformity over all chambers. The results of this global analysis are shown in Section 4.

4 Results

The results of the gas gain uniformity test here presented refer to six classes of chambers produced at CERN for the LHCb muon system. For this purpose, the gain over all pads of each chamber is measured. As in the read-out chain the output of two neighboring gaps is OR-ed, gaps #1 and #2 are grouped together and labeled as 'bi-gap 1', while gaps #3 and #4 are labeled as 'bi-gap 2'. The average normalized gas gain in each bi-gap is shown in Fig. 9 as a function of the chamber number in separate plots for different chamber types. In bi-gap 1 the average is calculated over the pads in the first and second gaps (filled markers) and in bi-gap 2 it is calculated over the pads in the third and fourth gaps (open markers). The inferior and superior limits of the error bars correspond respectively to the absolute minimum and maximum gas gain within the pads comprised in each bi-gap. All the values are renormalized by the average of the gas gain over all pads in all chambers of a given type. While M3R1 and M3R2 chambers were tested with a HV of 2650 V, all the other chambers have been tested with 2750 V. The gas gain variations are enhanced when the chamber is powered with higher high voltage. This can be noticed in Fig. 9 from the smaller error bars of the M3R1 and M3R2 chambers, when compared to the others.

The missing markers in the plots shown in Figure 9 correspond to chambers that have not been tested due to the reasons described in Table 3. Since the number of chambers constructed is about 10% to 20% higher than the actual number of chambers needed for the experiment, including spare ones, the chambers mentioned in Table 3 do not have any impact to the overall production scheme.

4.1 Classification

The specification for the gas gain uniformity per bi-gap requires a gain variation smaller than 30% for 95% of the surface [4]. In order to classify the performance of the chambers two intervals A and B around the average gas gain per gap have been defined:
interval A: $\overline{G}/\sqrt{2} \leq G(x,y,) \leq \sqrt{2} \cdot \overline{G}$ and
interval B: $\overline{G}/\sqrt{2} \leq G(x,y,) \leq \sqrt{2} \cdot \overline{G}$
where $\overline{G}$ is the average gas gain per bi-gap and $G(x,y,)$ is the gas gain on a certain position in x and y on the gap surface. The corresponding voltage range is $\pm$53 V and $\pm$84 V for interval A and B,

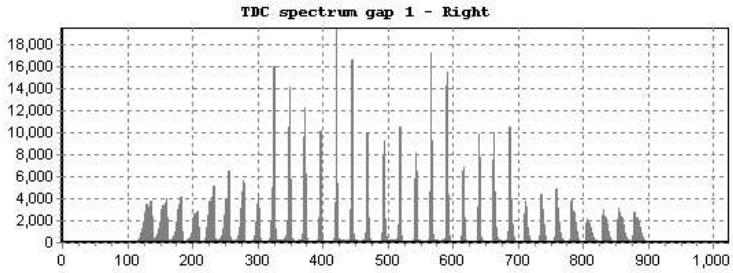

(a) The TDC spectrum for the right side.

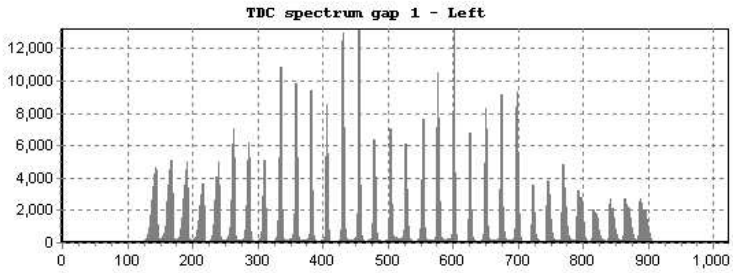

(b) The TDC spectrum for the left side.

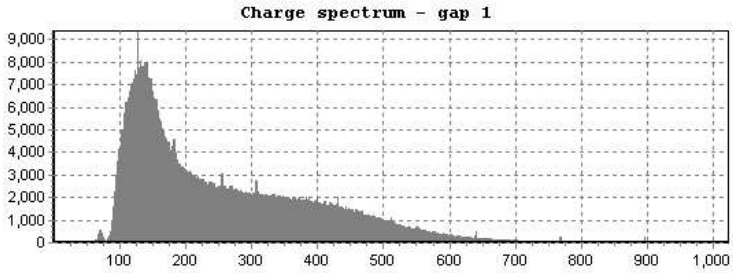

(c) Overall charge spectrum.

Figure 7: The TDC spectra from the cathodes and the ADC spectrum from the anodes are printed in the report for each gap.

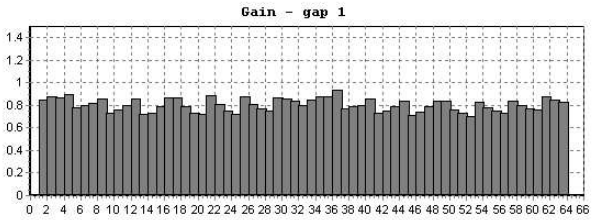

(a) Histogram of gain per pad in 1D.

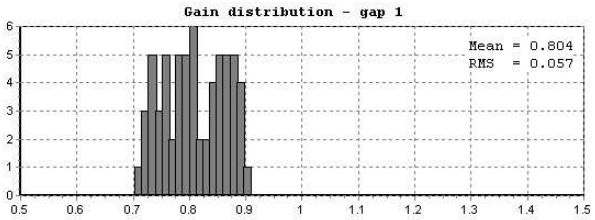

(b) The gain distribution.

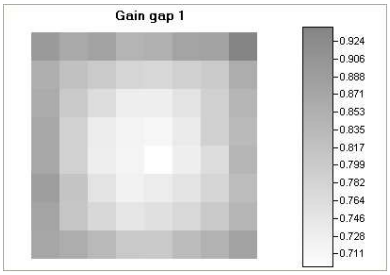

(c) Histogram of gain per pad in 2D.

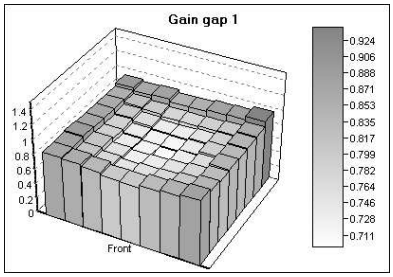

(d) Histogram of gain per pad in 3D.

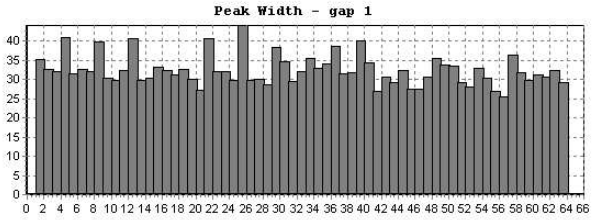

(e) Peak width as a function of pad number.

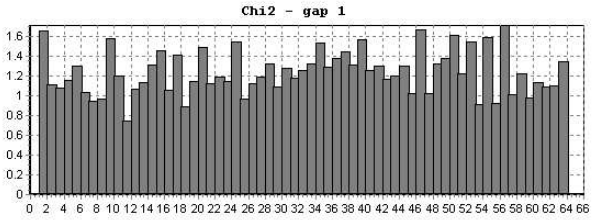

(f) χ^2 of the Gaussian fit as a funtion of the pad nr.

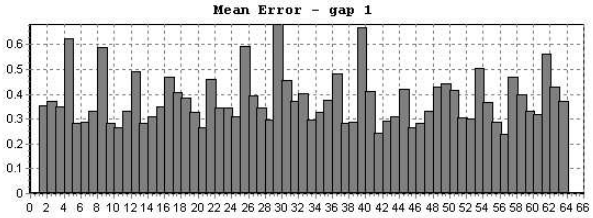

(g) Error on the peak mean value per pad.

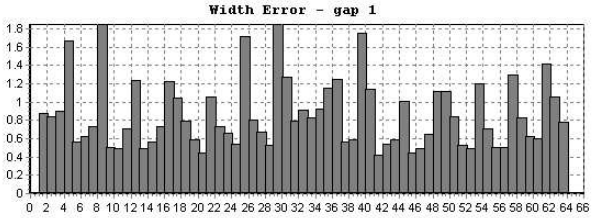

(h) Error on the width as a function of pad nr.

Figure 8: Gas gain distribution and analysis plots are created by the software and printed in the report file.

Table 3: Quality tests failures for chambers which do not appear on Figure 9. The pad connection to ground in chamber M4R1-01 was detected during the gas gain uniformity test.

Type	Number	Remarks
M2R1	07	Failed HV test
	13	Incomplete
M3R1	05	Being reassembled at the test time
	15	Used for ageing tests
M3R2	25	Failed HV test
M4R1	01	One pad connected to ground
	04	Failed gas leak test
M5R1	11	Failed gas Leak test

respectively [14].
The limits of the intervals A and B are indicated in figure 9 by two dotted and two solid lines, respectively.

According to these intervals, the bi-gaps can be classified into 3 categories:

- **A**: all the pads have the normalized gas gain within the limits of interval A;
- **B**: the variation of the normalized gas gain of the pads exceeds the limits of interval A, but all the pads have the normalized gas gain within the limits of interval B;
- **C**: the variation of the normalized gas gain of the pads exceeds the limits of interval B.

A chamber is classified as **Good** if the combination of the classification of both bi-gaps are **AA** (for bi-gap 1 and bi-gap 2), **AB** or **BA**, and as **Spare** if the classification is **BB**. A chamber with a gas gain variation larger than interval B is rejected and classified as **Failure** (**AC**, **CA**, **BC**, **CB** or **CC**).

4.2 HV dependency and correction

The classification of the different chamber geometries according to this criterium, denoted as "single HV classification", is shown in the second column of Table 4. However, it is important to note that the requirements above used to classify a chamber as **good** or **spare** are more stringent than necessary, since we will be able to set the HV for each gap separately. We could therefore analyse the gas gain uniformity separately for the different gaps in each chamber as we see in Fig. 9(f) for the chambers M5R1. The classification of each gap as **A**, **B** or **C** could be done with different limits, calculated with respect to the average over the pads in the corresponding gap (given by the markers) and not to the average over all the pads in all chambers of a given type. In this case, the requirement would be to have the inferior and superior limits of the error bars within the interval A. Then, chambers M5R1-1 and M5R1-2 would have all 4 gaps with the error bars contained within interval A of the average gas gain and would be classified as **good** chambers. We would need just to reduce the voltage applied to the third gap of M5R1-1 and M5R1-2 and increase the voltage applied to the fourth gap of M5R1-2. By increasing the voltage in the first and third gaps of chamber M5R1-15 we could also classify it as a **good** chamber, instead of classifying it as **spare**, as it was done when no correction to the HV is applied.

We then present, in the second column of Table 4, the classification of the chambers according to a criterium which considers that a different voltage can be applied to each gas gap, allowing the markers

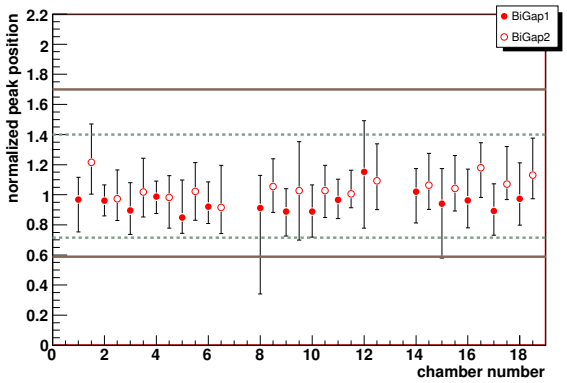

(a) M2R1

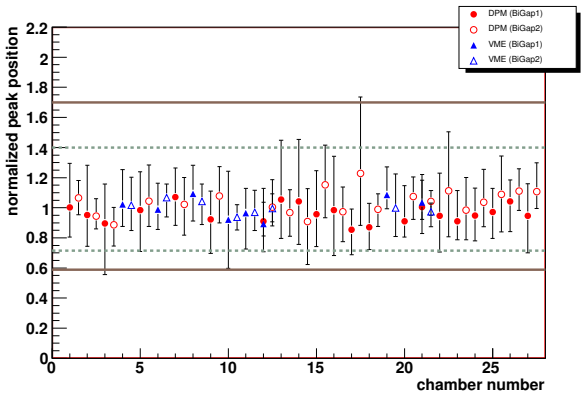

(b) M2R2

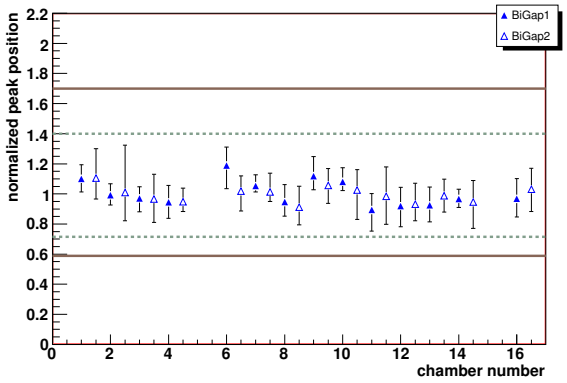

(c) M3R1

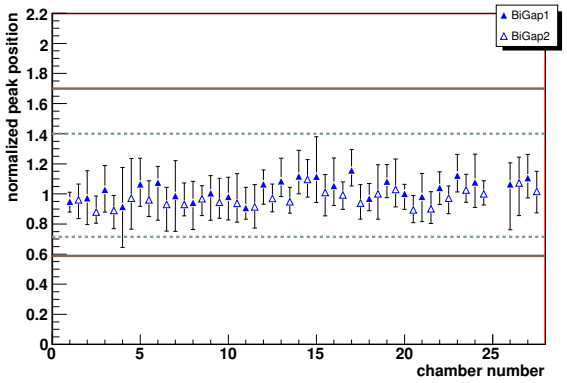

(d) M3R2

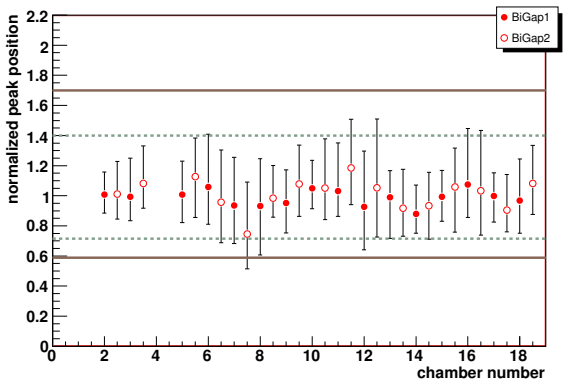

(e) M4R1

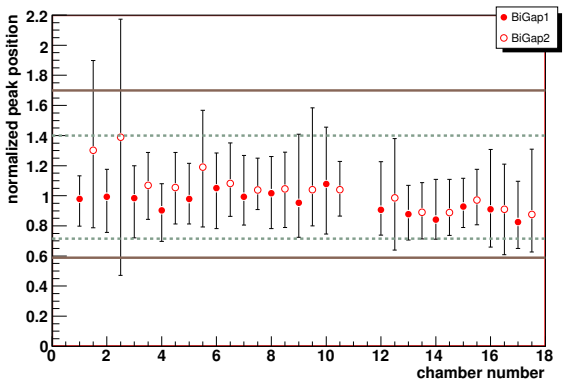

(f) M5R1

Figure 9: Normalized gas gain as a function of chamber number. Filled and empty symbols correspond to bi-gaps 1 and 2, respectively. Triangles are used for chambers tested with the new DAQ (DPM) and circles are used for the old system based on the VME standard. The error bars represent the minimum and maximum values of the normalized gas gain in the corresponding bi-gap.

corresponding to each bi-gap of Fig. 9 be displaced up or down in order to fit the error bars within the 2 gas gain limits. We denote this classification as "HV corrected classification". For M2R2, for example, we have a number of modifications to the detectors classification: M2R2-3 is classified as an **AA** chamber instead of **CA** when we increase the HV of bi-gap 1, M2R2-17 becomes **BA** instead of **BC** when we reduce the HV of the second bi-gap, M2R2-14 changes from **BB** to **BA** when the HV of bi-gap 2 is increased. In addition, chambers M2R2-9, M2R2-10 and M2R2-16 are reclassified as **AA** instead of **BA** when the HV of bi-gap 1 is increased. The total numbers of chambers needed for the experiment in each region, shown in Table 1, are achieved for all geometries, with any of the classification criteria.

Table 4: Number of chambers classified in the different categories.

Chamber Type	Single HV classification			HV corrected classification		
	Good	Spare	Failure	Good	Spare	Failure
M2R1	15	0	1	16	0	0
M2R2	24	1	2	27	0	0
M3R1	14	0	0	14	0	0
M3R2	26	0	0	26	0	0
M4R1	13	2	1	16	0	0
M5R1	12	3	2	17	0	0

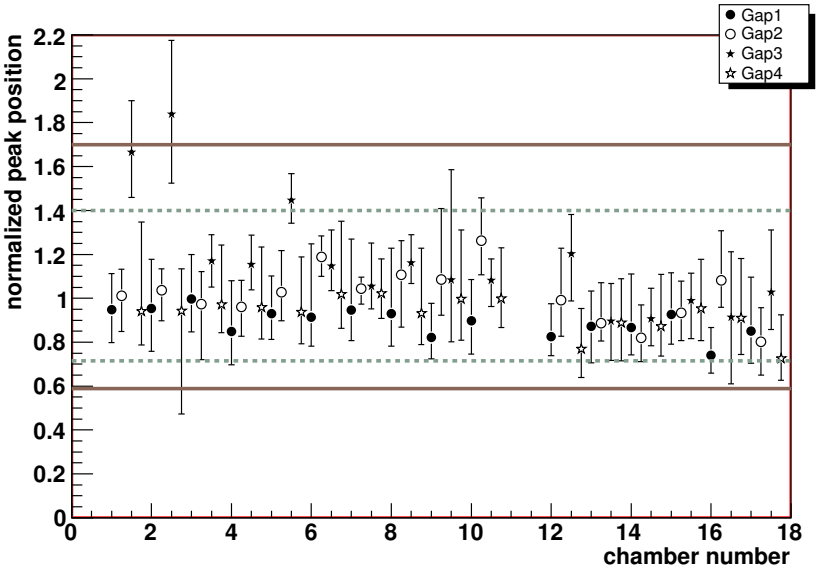

Figure 10: Average normalized gas gain as a function of chamber number for the different gas gaps.

4.3 Statistics

Even though no correction for different pressure and temperature conditions during the test has been applied to the data, the average normalized gas gain is rather uniform over the different chamber types, as can be seen from the mean and RMS values shown in Table 5. The maximum variation is seen for bi-gap 2 in the M5R1 chambers, dominated by the bad panel quality of chambers 1 and 2.

Table 5: Mean and RMS values of the normalized gas gain distributions for the different chamber types.

	Bigap 1		Bigap 2	
	Mean	RMS	Mean	RMS
M2R1	0,949	0,068	1,051	0,073
M2R2	0,978	0,066	1,022	0,069
M3R1	1,005	0,085	0,996	0,051
M3R2	1,032	0,067	0,968	0,053
M4R1	0,987	0,051	1,013	0,101
M5R1	0,951	0,069	1,049	0,140

We have also looked at the ratio $\mathcal{R}$ of the average gas gain over the 4 pads in the middle of the chamber to the average over the pads at the edge of the chamber. The distributions of $\mathcal{R}$ for the different chamber types are shown in Fig. 11 and their mean and RMS values are given in Table 6.

Table 6: Mean and RMS values of the $\mathcal{R}$ distributions.

	Gap 1		Gap 2		Gap 3		Gap 4	
	Mean	RMS	Mean	RMS	Mean	RMS	Mean	RMS
M2R1	0,96	0,05	0,91	0,11	0,89	0,07	0,83	0,07
M2R2	0,94	0,10	0,94	0,12	1,02	0,12	0,99	0,09
M3R1	0,92	0,04	0,99	0,03	1,03	0,07	0,91	0,04
M3R2	0,94	0,04	1,02	0,04	1,02	0,05	0,96	0,03
M4R1	0,95	0,06	0,91	0,19	0,90	0,15	0,91	0,14
M5R1	0,81	0,04	0,78	0,13	0,69	0,15	0,79	0,08
All Types	**0,92**	**0,08**	**0,94**	**0,13**	**0,94**	**0,15**	**0,92**	**0,11**

5 Conclusions

A gas gain uniformity test setup for the LHCb Muon chambers produced at CERN has been developed and the chambers have been tested with two DAQs: a VME based system and the dedicated data processing module (DPM) developed at CBPF. In figure 9(b) (M2R2 chambers) some units were tested with both the DPM and the VME-based setups. It may be noticed that the results are in good agreement, and this is an indication of the reliability of the method and of its implementation.

In total, we have tested 116 MWPC of 6 different geometries and have rejected only 6 of them due to non-uniformities in the gas gain, with a global criteria which assumes the same voltage applied to all gaps of all chambers. If only uniformity over the surface of each gap is required, all chambers pass the gas gain uniformity test.

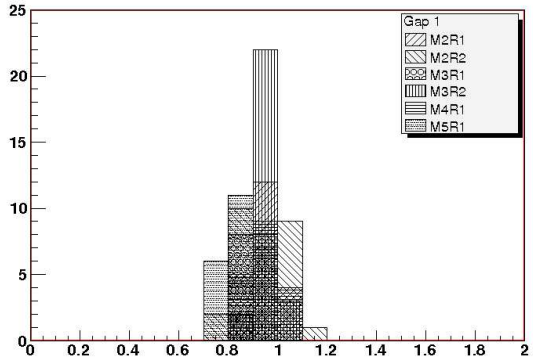

(a) Gap1

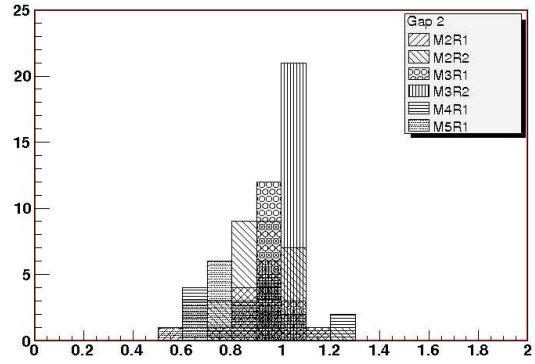

(b) Gap2

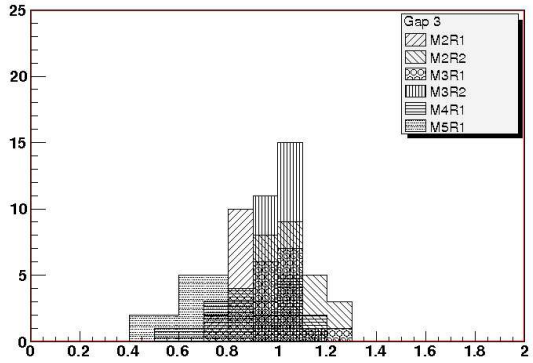

(c) Gap3

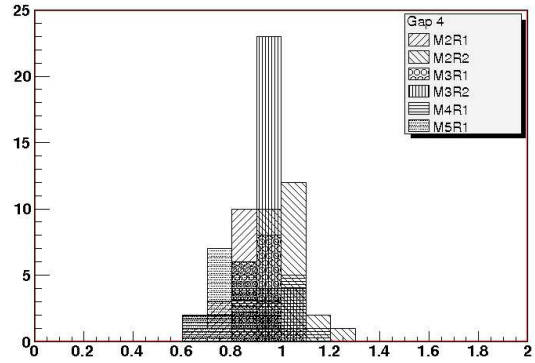

(d) Gap4

Figure 11: The distribution of $\mathcal{R}$ for the different gaps.

APPENDIX: Software Operation and Test Instructions

This appendix is intended to guide a new user to the test station to go through the testing procedure step by step. A detailed description of the software program MUCH is given, piloting the user through data acquisition and data analysis.

Calibration and Normalization

In order to initiate a gain uniformity test of a muon chamber, the first step is to follow a calibration procedure, which is divided in two operations: a) definition of an event filter by selection of the time window of the summed times of the delay line signals, b) adjustment of the pad positions in the timing spectrum, described below. It is supposed that the chamber is flushed with the operational gas mixture ($Ar/CO_2/CF_4$ 40:55:5), powered with nominal high voltage (2650V-2750V) and connected to the front end electronics driving the signals to the DAQ.

a Event filter by sum window

By using the *S*um button in the main window (also available in the Acquire menu) one switches the MUCH software to an acquisition mode where the delay time of the signals arriving on both ends of a delay line is summed instead of subtracted. This mechanism has been implemented in order to filter out events arriving out of time. Since the delay line has constant time length, the sum of the travel times of the signal on both ends is also constant. The sum spectrum should feature a peak centered at the delay line propagation time. Spurious events are distributed somewhat randomly outside the peak. By defining a region around the peak, an automatic filter is applied to the events during the data-taking. Only the events that fall inside that region, called ROI Time in the software, will be considered as valid events. The ones falling outside the region are rejected.

b Timing spectrum for pad profile adjustment

The pad positions in a cathode plane are identified from the measurement of the time differences (instead of the time sum) of signals traveling through the delay lines. The associated calibration is done by selecting the *D*elta button in the main window. For each tested chamber, the definition of each pad position must be done. By default, the MUCH software presents equally distributed time interval limits for all the pads. Usually, these limits do not perfectly match the actual position of the pads for a given chamber. In order to adjust the limits for each pad position, one must select the *S*can Pads button on the main window (also accessible through the Acquire menu) and manually define the limits by using the mouse.

The measurement of the anode amplitude is the most important one for testing the gas gain uniformity of the chamber, since the gain for each pad is directly obtained from the amplitude of the anode signal for events hitting this pad. It is necessary to implement a gain normalization in order to take into account the pre-amplifier gain, which is not necessarily the same for the 4 anode gaps in a chamber. This normalization is performed in the so-called Pulser mode. In order to switch to this mode, one should activate the Pulser Mode option in the Acquire menu. This changes the title of the bottom graphic window to Pulser gap X, where X is the active gap.

The normalization procedure makes use of a periodic signal (a square wave, generated externally by a waveform generator) which is directly injected into the anode preamplifiers. The amplitude

of this test signal emulates the pulse height of the mean anode amplitude of an arbitrarily selected chamber. Once the standard pulse amplitude has been defined, it is of course used as the parameter to compare all the chambers of a given type. By using this method, different chambers may be compared in what concerns the gain uniformity.

After setting the acquisition to the Pulser mode and adjusting the amplitude of the test signal, one can start an acquisition for normalization purpose. The data acquisition is started with the *S*tart button and finished with the *S*top button. Depending on the frequency of the test signal, a few seconds are enough to obtain a well-defined histogram in the Pulser graphic window. After the histogram is built, one should apply a Gaussian fitting to the distribution. This can be done by selecting the option Analysis→ROI Pulser. The resulting mean value is used for normalizing the gain over all pads in a gap.

Given an event counting rate, there is a probability that an event will be detected while the previous one has not yet been completely neutralized in the chamber. This causes piling up of signals, which translates into an average base-line at the pre-amplifier output which is not at the zero volts level. This offset is the actual base-line amplitude, and has to be corrected for when the amplitude histogram is obtained. In order to obtain the base-line distribution, the Baseline acquisition mode button is selected. The histogram is then filled with anode signals that not belonging to a triggered event. For this purpose the trigger of a real event in one gap is used to read out the signals from the other three gaps. A Gaussian fit has to be applied to the obtained profile, just as explained for the Pulser mode. The peak position is obtained and the chamber gas gain is corrected for by this bias value.

Acquisition

After the initial calibration procedures data-taking can be started. In order to test a chamber, the acquisition mode must be set to *Delta*, i.e., the measurement of time differences of delay line signals must be activated. This is done by pressing the corresponding button on the main window.

A new data acquisition can be started by pressing the *Start* button on the main window. The current data acquisition can be finished by pressing the *Stop* button. The *Clear* button removes all the data stored in the memories, as well as the contents of the graphic windows (TDC and ADC). If the sequence *Start-Stop-Start* is done without activation of the *Clear* button, the data acquisition starts from the data previously stored in the memories and shown in the graphic windows. In the Automatic Acquisition mode a time period can be selected to stop data acquisition automatically.

Analysis tools

Besides calibration, normalization and acquisition facilities, MUCH provides tools for fitting and analyzing the acquired data. The following items describe the main features related to fitting and analysis in the MUCH environment.

a Energy spectrum

In order to analyze the peak of the anode signal distribution for the whole chamber, one spectrum has to be defined for each pad. The peak position is related to the gas gain of the chamber in each pad. The process for fitting the energy spectra of all the pads, in a given gap, can be done by defining a region of interest over the global spectrum, and then pressing the *Fit All Pads* button. This region can be defined by using the *ROI Pad* button. The global spectrum can be viewed in the ADC graphic when no pad is selected. After this global fitting, one should

proceed to make fine adjustments in the resulting fit for each of the pads. The energy spectrum for every pad in the chamber can be viewed in the ADC graphic window. The first step now, if one intends to improve the fit quality, is to re-define the region of interest previously selected through the global spectrum. With the energy spectrum active for a given pad, one can use again the *ROI Pad* button, and select the region of interest over the spectrum. Only after that, by pressing the *Fit Pad* button, the fitting tool will calculate the best Gaussian fit for the active distribution. If the fitting process is successful, the mean peak for the pad and related fitting parameters (standard deviation, chi-square, etc.) are automatically stored in memory.

b Gain homogeneity visualization

In order to provide visual inspection of the results, MUCH features the Analysis window, which is activated by pressing the option Fit Results on the Analysis menu. This window exhibits a three-dimensional view of the results obtained from the energy spectrum for each pad of the chamber. One of the results that can be viewed is the Normalized Mean, as shown in Figure 12.

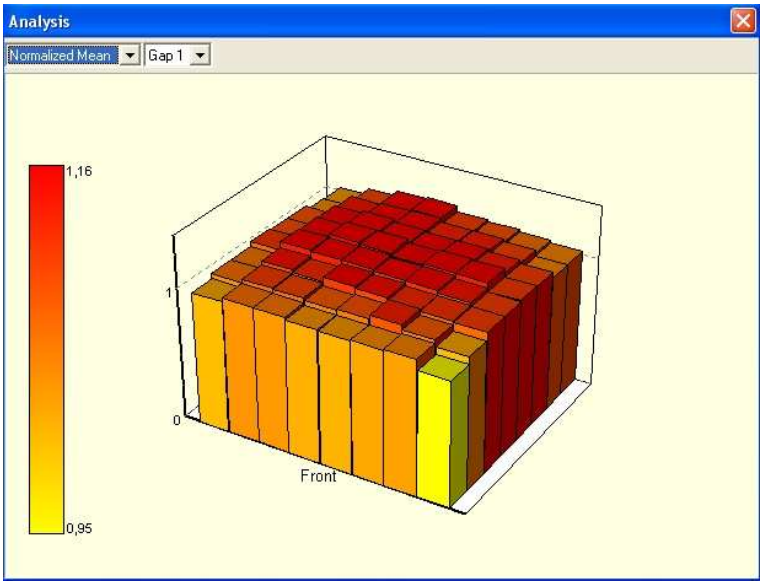

Figure 12: Capture of the Analysis window, showing a 3D-view of the gain uniformity.

c Report generation

Once the tasks of data acquisition, fitting and analysis have been concluded, one can generate a complete report containing different views of all the results. The report is produced by selecting the option Report File in the menu Analysis. When that option is selected, a window called Log Header is opened, presenting some fields that should be filled in with general information on the test conditions. By pressing the *OK* button on this window, the MUCH software generates and opens a document file (MS-Word format) containing the report. The report is not created in case there are irregular results. These errors can be viewed in the Analysis window. One possible irregularity is a negative value for the gain or some other parameter for one or more pads. This is due to erroneous fitting.

d Saving the acquisition

The entire acquisition, including pad identification, energy spectrum, base line, pulser acquisition and fitting results, can be saved by selecting the option Save in the *File* menu. All the information processed since the start of the application is saved in a single file. This file, with the extension '.tdf', is specific of the MUCH software environment.

References

[1] LHCb Collaboration, *LHCb Muon System TDR*, CERN-LHCC-2001-010, May 2001.

[2] LHCb Collaboration, *LHCb Muon System TDR Addendum 1*, CERN-LHCC-2003-002, January 2003.
LHCb Collaboration, *LHCb Muon System TDR Addendum 2*, CERN-LHCC-2005-012, April 2005.

[3] http://lhcb-muon.web.cern.ch/lhcb-muon/Ch.htm
W. Riegler, *Crosstalk, Cathode Structure and Electrical Parameters of the MWPCs for the LHCb Muon System*, LHCb Muon 2000-061, April 2003.

[4] A. F. Barbosa *et al.*, *Production and quality control of MWPC for the LHCb Muon System at CERN*, IEEE Transactions on Nuclear Science, **53**:1, February 2006.

[5] A. F. Barbosa, *A test station for Muon MWPC*, LHCb 2002-047, October 2002.

[6] A. F. Barbosa, L. Manhães de Andrade Filho, E. Polycarpo, *Characterization of the MWPC test station for the production sites*, LHCb 2005-011, September 2004.

[7] Information Technology Division, *PAW Reference Guide - CERN Program Library Long Writeup Q121*, January 1999.

[8] http://www.ti.com (OPA657 datasheet)

[9] A. F. Barbosa, Roberto da Silva, *A fast voltage preamplifier for use with MWPCs*, Nucl. Inst. Meth. A **555**, 93-100, 2005.

[10] http://www.analog.com (AD9238 datasheet)

[11] http://www.analog.com (AD3138 datasheet)

[12] http://www.acam.de (F1 datasheet, scientific version)

[13] http://wwwcompass.cern.ch

[14] S. de Capua *Study of Gas Gain Uniformity of the LHCb Muon System MWPCs using Cosmic Rays*, LHCb-Muon 2006-010, March 2006.